minerals

MDPI

Article

Interactive Relationship between Cementitious Materials and Acid Mine Drainage: Their Effects on Chromium Cr(VI) Removal

Ayanda N. Shabalala [1,2,*] and Moses Basitere [3]

[1] School of Biology and Environmental Sciences, University of Mpumalanga, Mbombela 1200, South Africa
[2] Civil Engineering Science, University of Johannesburg, P.O. Box 524, Auckland Park 2006, South Africa
[3] Bioresource Engineering Research Group (BioERG), Department of Chemical Engineering, Cape Peninsula University of Technology, P.O. Box 652, Cape Town 8000, South Africa; Basiterem@cput.ac.za
* Correspondence: Ayanda.Shabalala@ump.ac.za

Received: 16 August 2020; Accepted: 14 September 2020; Published: 22 October 2020

Abstract: Elevated hexavalent chromium (Cr(VI)) levels in pervious concrete may undermine its successful application in water treatment. Portland cement CEM I 52.5R (CEM I), coal fly ash (FA), natural zeolite and ground granulated blast-furnace slag (GGBS) were evaluated as adsorbents for removal of Cr(VI) from acid mine drainage (AMD). Adsorption experiments were conducted at dosages of 6, 10, 30 and 60 g of adsorbent in 200 mL of AMD, while the mixing contact time was varied from 15 to 300 min. It was found that the use of CEM1 and FA adsorbents strongly increased the Cr(VI) concentration in AMD. Conversely, zeolite and GGBS removed up to 76% and 100% of Cr(VI) from AMD, respectively, upon their use at dosages of at least 10 g of the adsorbent. Freundlich isotherm was found better fitted with a high correlation coefficient (R^2 = 0.998 for zeolite and 0.973 for GGBS) than to the Langmuir model (R^2 = 0.965 for zeolite and 0.955 for GGBS). Adsorption and ion exchange seem to be active mechanisms for the Cr(VI) removal. These results suggest that zeolite and GGBS can be considered as partial cement replacement materials for effective reduction or removal of Cr(VI) from the treated water.

Keywords: adsorption; pervious concrete; hexavalent chromium; cementitious materials; acid mine drainage

1. Introduction

Chromium exists in various oxidation states ranging from Cr(II) to Cr(VI). Among these states, Cr(III) and Cr(VI) are the most common and most stable species [1,2]. Different species of chromium originate from its industrial applications, as well as incineration facilities, cement, contaminated landfill, asbestos lining erosion, tobacco smoke, topsoil and rocks [3]. The resulting industrial waste materials containing Cr(VI) are often disposed of into the environment, leading to contamination of natural water resources and soils, amongst others. The Cr(VI) varieties found in water are $Cr_2O_7^{2-}$, CrO_4^{2-}, H_2CrO_4, and $HCrO_4^-$ [4]. Of these, the variety that becomes prevalent in aqueous solution is determined by pH of the solution, chromium concentration, the presence of oxidising and reducing compounds, and the redox potential [3]. $Cr_2O_7^{2-}$ and $HCrO_4^-$ are the predominant varieties at the pH range of 2.0 to 6.0. At pH above 6.0, the dominant species is CrO_4^{2-} [3,4]. Equations (1) and (3) show the dissolved forms of Cr(VI) typically present in solution, as determined by the solution pH level.

$$H_2CrO_4 \rightarrow H^+ + HCrO_4^- \text{ (pH 2.0 to 6.0)} \quad (1)$$

$$2HCrO_4^- \rightarrow Cr_2O_7^{2-} + H_2O \text{ (pH 2.0 to 6.0)} \quad (2)$$

$$HCrO_4^- \rightarrow H^+ + CrO_4^{2-} \ (pH > 6) \quad (3)$$

Fly ash (FA), ground granulated blast-furnace slag (GGBS) and natural zeolite, all exhibit pozzolanic properties and are conventionally used in concrete as partial cement replacement materials for improvement of durability, among other beneficial effects [5–9]. Various researchers have demonstrated the potential of FA as an effective adsorbent for wastewater treatment [10–12]. Partial replacement of pervious concrete with FA has been shown to improve the workability of fresh concrete and the mechanical strength and durability of hardened concrete [13]. Fly ash can be utilised for a cleaner production of pervious concrete possessing compatible hydrological property and pollution control potential, compared to the ordinary pervious concrete [14]. Zeolites are low-cost ion exchangers that have been used as adsorbents for removal of heavy metals including chromium, etc., [15,16] from polluted water. Due to their net negative charge, zeolites have a strong affinity for transition metal cations. Zeolites are often abundantly available in natural deposits; they also exhibit high chemical stability [17–19]. A recent investigation by Bae et al. [20] found that the replacement of Portland cement with a small amount of only 5 wt% GGBS, significantly reduced the dissolved Cr(VI) in aqueous solution. There was complete sorption and reduction of Cr(VI) to Cr(III) using GGBS in a $Ca(OH)_2$ solution of pH > 12.5.

Cr(VI) is an extremely toxic chromium species that is known to cause severe environmental and health problems [21] to human, animal, and aquatic life systems. Such adverse health effects of Cr(VI) include contact dermatitis, lung carcinoma, diarrhoea, ulcers, kidney failure, liver damage, and other diseases of the gastrointestinal organs [3,22–25]. Not only is Cr(VI) highly carcinogenic and mutagenic, it is also known to cause birth defects [3]. Inhalation of Cr(VI) can cause asthma, bronchitis, pneumonitis, inflammation of the larynx and liver, perforation of the nasal septum, and increased risks of cancer of the respiratory system [21–23,26]. Cr(VI) is classified as a Group 1 human carcinogen by the International Agency for Research on Cancer [27] and was identified by the United States Environmental Protection Agency (USEPA) as one of the 17 chemicals that pose a threat to human life [28]. The World Health Organization specifies 0.05 mg/L as the maximum permissible limit of Cr(VI) in water for domestic use [29]. Given the severe health hazards of Cr(VI), it is a crucial necessity to ensure its removal from any sources that may lead to its direct contact with life systems.

The conventional approach for Cr(VI) removal from wastewater involves its reduction from the hexavalent to the trivalent state, followed by its precipitation as Cr(III) hydroxide, by means of physical, chemical, or bioremediation methods. Physical methods employ the physico-chemical properties of materials to achieve chromium remediation through various mechanisms including adsorption, electrodialysis, membrane filtration, photocatalysis, amongst others. Chemical remediation utilises chemicals such as sulphur dioxide, sodium metabisulfite, ferrous sulfate, sodium sulfite, barium sulfite, lime and limestone for the reduction of Cr(VI) to Cr(III). Bioremediation refers to the use of living organisms including bacteria, fungi, yeast, algae, and plants to remove pollutants [3]. The problems associated with use of physico-chemical methods for Cr(IV) removal include the high operating costs of the treatment, high energy consumption, excessive use of chemicals, generation of toxic sludge and air pollution resulting from the use of sulphur-based reducing agents [22,30]. These reductants generate SO_2 or H_2S under strong acidic conditions and emit an unpleasant odour, both of which seriously affect the health of workers [10]. Although bioremediation for chromium removal from wastewater may show good performance under laboratory testing, it is not often suitable for large-scale field systems, since the living organisms utilised for the treatments are not naturally available in abundance and have to be grown or cultured [1].

Adsorption offers the benefits of a clean, cost-effective, easily controlled, efficient process [4]. Natural bio-adsorbents, such as sawdust, have been successfully used for adsorption of Cr(VI). However, low adsorption capacities, high chemical, and biological oxygen demand, as well as leaching of organic components remain the main drawbacks of applying biosorbents [31]. Natural polymer-based adsorbents offer the benefits of low-cost, high effectiveness and regeneration potential. Examples of natural polymer-based adsorbents are chitin [32], cellulose [33] and chitosan [34]. Chitosan contains

chemical functional groups, such as NH_2 and OH, while cellulose is mostly dominated by OH^- and CHO^- groups that can aid in trace metal sequestration and complexation. [31]. Carbon-based adsorbents, such as activated carbon [35] and biochar [36], possess a vast network of internal pores by which they have high surface areas and become excellent adsorbents [37]. Other adsorbents that have shown varying success in Cr(VI) adsorption include bentonite clay, zero-valent iron, bauxite and iron oxide nanoparticles [38–41]. However, most of the adsorbents show limitations in adsorption capacity and are often not re-usable [4].

Due to its particle retention capacity during filtration, concrete products can function as pollution sink [42,43]. Contaminants, such as heavy metals and organic compounds, are absorbed into the internal concrete body and are eliminated from the runoff. Other potential benefits of using this type of pavement include recharging of groundwater, saving of water by recycling, and prevention of pollution [44]. Reductions in suspended solids, biochemical oxygen demand, chemical oxygen demand and ammonia levels in surface runoffs demonstrate the high treatment efficiency of pervious pavement systems [45]. It can also lead to a reduction in oil, grease, and petroleum products, from the water effluent drained through pervious concrete [43]. Several recent studies [43–49] have shown pervious concrete to be a promising alternative reactive material for the treatment of acid mine drainage (AMD). However, elevated Cr(VI) levels in the treated water arising from the use of cement and FA in pervious concrete, may potentially undermine concrete's successful application in water treatment. Chromium in cement is found primarily in the form of Cr(III), while Cr(IV), Cr(V) and Cr(VI) may exist in smaller quantities [50,51]. The oxidising environment in kilns under the typically high operating temperatures of up to 1450 °C, transforms the Cr(III) found in the materials into hexavalent state [21]. Cr(VI) in cement emanates from different sources including some refractory bricks, raw materials, fuels, and the chromium alloys used in grinding mills. The release of Cr(VI) into the environment when cement or concrete products are exposed to water, soil and air, may result in a threat to environmental safety and human health.

In the present study, adsorption experiments were conducted on Portland cement CEM I 52.5R (CEM I), FA, natural zeolite and GGBS, to assess their effects as adsorbents for effective removal of Cr(VI) from AMD. The present study aimed at identifying effective adsorbent(s) that may be incorporated into pervious concrete for removal of Cr(VI) from the concrete-treated AMD. Batch adsorption experiments were implemented under different criterions, including adsorbent dosage, contact time, and pH. Fourier-transform infrared spectroscopy (FTIR), X-ray powder diffraction (XRD), and scanning electron microscopy-energy-dispersive X-ray spectroscopy (SEM-EDS), were used to investigate the physico-chemical properties of the adsorbents.

2. Materials and Methods

Naturally occurring AMD was obtained from an abandoned coal mine for use in the experiment. The AMD was collected from its discharge source using high-density polyethylene containers and transported to the laboratory for use in the experiments. The pH of the raw AMD was 3.01, while its composition [47] showed high concentrations of Ca (470 mg/L), Mg (214 mg/L), Na (3061 mg/L), Fe (9 mg/L), Al (6 mg/L) and SO_4 (2870 mg/L). The concentration of Cr(VI) in the raw AMD was 0.042 mg/L.

Adsorption tests were conducted on CEM I; Class F, FA; natural zeolite and GGBS as adsorbents for Cr(VI) removal from AMD. The CEM I, FA, and zeolite materials used, were obtained from AfriSam SA (Pty) Ltd. (Roodepoort, South Africa), Ash Resources SA (Pty) Ltd. (Edenvale, South Africa), and Serina Trading (Pty) Ltd. (Heidelberg, South Africa), respectively. GGBS was also supplied by AfriSam SA (Pty) Ltd. Phase identification of the unreacted and reacted adsorbents was carried out using X-ray diffraction (XRD) (Malvern Panalytical Ltd., Malvern, UK) at a scan rate of 0.02°, 2-theta per minute using a Pan Analytical X-ray X'pert PRO diffractometer (Malvern Panalytical (Pty) Ltd., Malvern, UK). The XRD instrument consisted of a PW3830 X-ray generator operated (Malvern Panalytical (Pty) Ltd., Malvern, UK) at 40 kV, 40 mA and a copper X-ray tube. Morphological

characterisation of the adsorbents was conducted by scan electron microscopy–energy dispersive spectrometer (SEM–EDS) (TESCAN VEGA 3 SEM, (Tescan Orsay Holding, Brno, Czech Republic). The SEM samples were cross-section cut and dried under vacuum. Then, the samples were fixed on the aluminium stub and sputter-coated with gold particle. An AZtec energy dispersive spectrometer (EDS, Oxford instruments, Abingdon, UK) was employed to determine elemental composition of phases in the samples. Functional groups were determined using BX-II PerkinElmer FTIR (Perkin Elmer, Waltham, MA, USA) equipped with the universal attenuated total reflectance (ATR) diamond crystal. Then, 0.5 g of the adsorbent is placed into contact with the ATR sampling crystal and subjected to IR radiation. Some of this radiation is absorbed by the sample and is measured as an infrared spectrum. The ATR technique gave a spectral range from 4000 to 400 cm^{-1}.

The concentration of Cr(VI) in AMD was determined using a WLAB/046/Discrete Chromium Analyser (Skalar Analytical B.V., Breda, The Netherlands) based on the American Public Health Association, Standard Method 3500 Cr B Colorimetric Method [52]. The AMD sample was reacted with diphenylcarbazide under acid conditions (pH of 2 ± 0.5). Cr(VI) produces a red-violet colour which is measured photometrically at wavelength 540 nm. The limit of detection (LOD) was 0.0048 mg/L. The amount of Cr(VI) contaminant adsorbed (q_e) in mg/g and the removal efficiency (RE) levels were calculated using Equations (4) and (5), respectively [53].

$$q_e = (C_o - C_e) \times \frac{V}{m} \quad (4)$$

$$RE\,(\%) = \frac{C_o - C_e}{C_o} \times 100 \quad (5)$$

where C_o is the initial concentration of the contaminant in raw AMD (mg/L), C_e is the equilibrium concentration of the contaminant (mg/L), V is the volume of AMD (litres), m is the mass of the adsorbent (g).

Batch adsorption experiments were carried out in 500 mL graduated borosilicate glass beakers. The experiments were performed using 200 mL of AMD containing 0.042 mg L^{-1} of Cr(VI) at 25 °C and 150 rpm for 300 min. Adsorption efficiency of Cr(VI) by the adsorbents was studied by varying the adsorbent dosage. The following dosages were used for the individual adsorbents: 6.0, 10.0, 30.0 and 60.0 g. A high precision electrical balance (Ohaus Scout Pro Portable Electronic Balance) was used for weighing. The mixture was filtered through a 0.45 µm Whatman® PTFE membrane filter. Treated AMD samples were transferred into 200 mL plastic vials. The pH, Electrical Conductivity (EC) and Total Dissolved Solids (TDS) were measured using a digital pH meter (MP-103 microprocessor-based pH/mV/Temp tester (Gondo electronic Co. Ltd., Taipei, Taiwan). The pH electrode used was calibrated using standard NIST-traceable pH 2.0, 4.0, 7.0 and 10.0 buffers. Treated AMD samples were stored in a refrigerator set at a constant temperature of 3 °C before the determination of Cr(VI) concentration.

Column tests were conducted to determine the leaching behaviour of Cr(VI) from CEM I, FA and GGBS. Pervious concrete was made, using 6.7 mm granite aggregate and Portland cement consisting of CEM I 52.5R (CEM I) alone or CEM I with 30% fly ash or CEM I with 50% GGBS. A mixture of 0.27 water/cementitious ratio was used. The mixture was placed into standard 100 mm cube moulds and then compacted using a vibrating table. The fresh concrete cubes were de-moulded after about 24 h and placed in a water curing bath until 28 days of age [47]. Four concrete cubes of CEM I, 30%FA and 50% GGBS were placed in separate columns. The columns used in this study were 500 mm in height, and had an internal diameter of 100 mm. An AMD sample was pumped at a flow rate of 0.35 mL/min. Leachate samples were collected daily for the first three months, then once every third day, and thereafter once a week for a total of 320 days. The concentrations of Cr(VI) were determined using WLAB/046/Discrete Chromium Analyser.

Langmuir and Freundlich isotherms are the most commonly used models for adsorption studies. Equation (6) gives the Langmuir model which can also be expressed in the linearised form given

in Equation (7). By plotting the graphs of adsorption data as $1/q_e$ versus $1/C_e$, a trendline is obtained whose slope and intercept is used to directly determine the values of q_m and K, based on Equation (7) [26,54].

$$q_e = \frac{q_m K C_e}{1 + K C_e} \quad (6)$$

$$\frac{1}{q_e} = \frac{1}{K q_m} \times \frac{1}{C_e} + \frac{1}{q_m} \quad (7)$$

where q_e (mg/g) is the amount of contaminant adsorbed (adsorbate) at the equilibrium concentration, C_e (mg/L) is the equilibrium concentration of adsorbate, q_m (mg/g) represents the maximum monolayer adsorption capacity, and K (l/mg) is the Langmuir constant related to energy of adsorption and the affinity of the binding sites. The essential characteristics of the Langmuir isotherm can be expressed in terms of a dimensionless constant called the separation factor, R_L, as shown in Equation (8) [33]:

$$R_L = \frac{1}{1 + K_L C_0} \quad (8)$$

where C_0 is the maximum initial concentration of the adsorbate (heavy metal ion) and K_L(L/mg) is a constant related to the affinity of the binding sites. When the values of $R_L > 1$, it is an indicator that adsorption is unfavourable, $R_L = 1$ indicates linear adsorption, favourable when $0 < R_L < 1$ and irreversible when $R_L = 0$.

The Freundlich isotherm of Equation (9) accounts for multilayer physico-chemical adsorption on heterogeneous surfaces and can be expressed in a linearised form as given in Equation (10).

$$q_e = K_F \cdot C_e^{\frac{1}{n}} \quad (9)$$

where C_e is the concentration of the adsorbate at equilibrium (mg/L), K_F is the Freundlich capacity factor, and 1/n is the intensity. The latter two parameters are obtained by fitting Equation (9) to graphs of adsorption data plotted as $\log q_e$ versus $\log C_e$.

$$\log q_e = \frac{1}{n} \log C_e + \log K_F \quad (10)$$

3. Results

3.1. Characterisation of Adsorbents

Chemical analyses of the adsorbents were performed using X-ray fluorescence (XRF, Bruker, Karlsruhe, Germany), giving the chemical compositions shown in Table 1. The high CaO and SiO_2 contents of CEM I are responsible for strength development in concretes. FA and zeolite are pozzolanic materials composed of mainly amorphous aluminosilicate elements, while GGBS is a latent hydraulic cement exhibiting both pozzolanic and cement properties. It can be seen in Table 1 that GGBS had intermediate levels of all the three oxides comprising CaO, SiO_2 and Al_2O_3. The typical concentrations of total chromium Cr_2O_3 concentrations in South African CEM I, FA, GGBS are 102, 200 and 193 ppm, respectively [51,55,56]. Potgieter et al. [51] also reported that 30 to 80% of the total chromium in cement is Cr(VI) of which 8 to 26% is leachable or water soluble. A study by Eštoková et al. [57] stated that the average concentrations of the total chromium in cements vary from 178.5 to 257.3 mg per kg of cement while the average concentrations of hexavalent chromium ranged from 0.5 to 2.46 mg/kg.

Table 1. Chemical compositions of Portland cement (CEM I), fly ash (FA), natural zeolite and ground granulated blast-furnace slag (GGBS). LOI = Loss on Ignition.

Adsorbent	SiO_2	Al_2O_3	CaO	Fe_2O_3	MgO	TiO_2	Mn_2O_3	SO_3	Na_2O_3	K_2O	LOI
CEM I (%)	21.9	4.75	65.44	3.68	2.17	0.49	0.40	1.92	0.17	0.25	1.57
FA (%)	50.32	24.57	7.31	5.91	1.83	1.53	0.05	0.16	0.16	0.76	5.59
Zeolite (%)	58.12	11.44	1.01	1.57	1.30	0.12		0.18	2.03	1.44	22.36
GGBS (%)	37.03	13.39	36.62	0.61	8.00	0.63	0.87	2.31	0.23	1.11	0.19

3.2. *Cr(VI) Adsorption Tests*

3.2.1. Effect of Adsorbent Dosage

It can be seen in Figure 1a that CEM I showed an increase in Cr(VI) concentration with increase in dosage of the adsorbent, attaining a maximum concentration of 4.27 mg/L at the dosage of 60 g of the adsorbent in 200 mL of AMD. As mentioned in Section 1, chromium is present in Portland cement as an impurity. In recent studies [47–49], it was reported that mine water treated with pervious concrete exhibited high levels of Cr(VI) owing to leaching from the cement and fly ash materials used in PERVC mixtures. FA also increased the concentration of Cr(VI) in AMD, but to a lesser extent than CEM I. Cr(VI) increased from 0.042 mg/L in raw AMD to 0.211 mg/L and 0.535 mg/L when 6 g and 60 g of FA were mixed with 200 mL of AMD, respectively. Clearly, both CEM I and FA increased the Cr(VI) concentration from 0.042 mg/L in raw AMD to levels exceeding the maximum permissible limits of 0.1 mg/L and 0.05 mg/L, in the treated AMD, specified in Environmental Protection Agency (EPA) [58] and World Health Organization (WHO) [29] or National Water Act (NWA) [59], respectively. The observed elevation of Cr(VI) in the AMD following its treatment using CEM I or FA, is attributed to leaching of the chromium present in the powder materials, into the polluted mine water [51]. Interestingly, Cr(VI) in AMD was removed or significantly reduced when the zeolite and GGBS adsorbents were used, as seen in Figure 1b. The Cr(VI) concentration in AMD reduced with an increase in the GGBS dosage, achieving complete removal at the dosage of 30 g of the adsorbent in 200 mL of AMD. Bae et al. [20] suggested that chromium removal by GGBS, could be attributed to the dissolved anions from slag, which may serve as reducing agents to transform Cr(VI) to Cr(III). Additionally, in the present study, a small dosage of only 6 g of zeolite in 200 mL of AMD, was sufficient for effective reduction of the Cr(VI) concentration level.

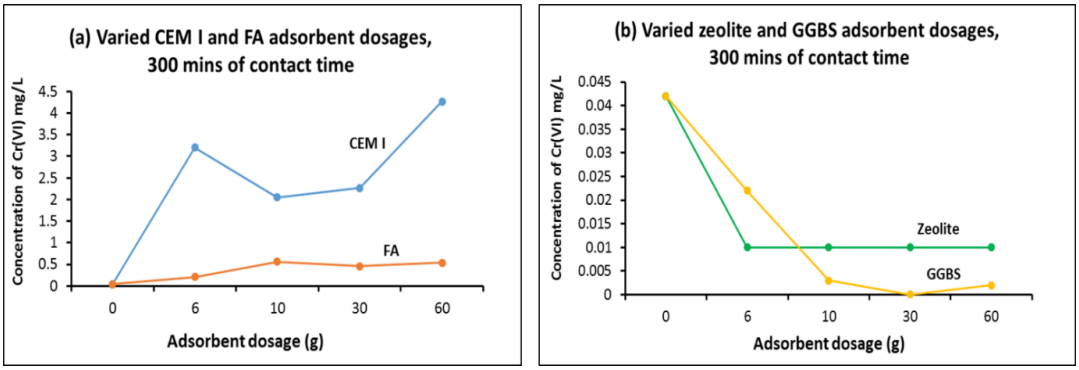

Figure 1. Effect of dosage on adsorption of Cr(VI) by various adsorbents after 300 mins of contact time with the AMD: (**a**) CEM I and FA adsorbents; (**b**) Zeolite and GGBS adsorbents.

3.2.2. Effect of Contact Time

In the experiment, contact time between the adsorbent and AMD was varied from 15 to 300 min. The CEM I and FA adsorbents strongly increased the Cr(VI) concentration in AMD, more so with longer contact time, as seen in Figure 2a. Notably for FA, there was no significant change in the concentration of Cr(VI) after 15 min of contact time. After 300 min of contact, the Cr(VI) concentration had risen

from 0.042 mg/L in raw AMD to equilibrium levels of 2.05 mg/L for CEM I and 0.558 mg/L for FA, both of which exceed the maximum limits of 0.10 and 0.05 mg/L specified in EPA [58] and NWA [59] or WHO [29], respectively. It can be seen in Figure 2b that zeolite and GGBS showed rapid removal of Cr(VI) at the early ages, with near complete removal of the contaminant occurring within 15 min of contact between the adsorbent and AMD. The Cr(VI) concentration was reduced from 0.042 mg/L in raw AMD to equilibrium concentrations 0.0107 mg/L and 0.002 mg/L after the water treatment using zeolite and GGBS, respectively. There was no significant change in concentration of Cr(VI) after 15 min of contact, indicating that the adsorption phase had reached equilibrium. Evidently, a minimum contact time of 15 min was required for removal or reduction of Cr(VI) by zeolite or GGBS to low concentration levels that meet the limits specified in national water standards [58,59].

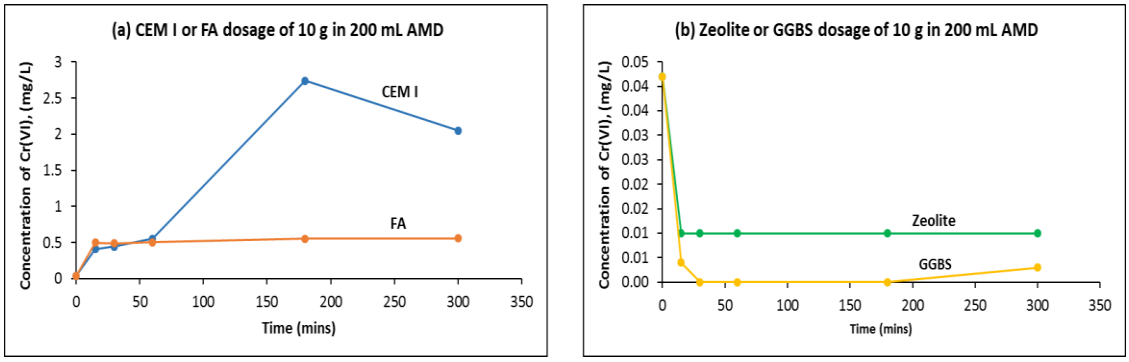

Figure 2. Effects of contact time on adsorption of Cr(VI) by the various adsorbents: (**a**) CEM I and FA adsorbents; (**b**) Zeolite and GGBS adsorbents.

3.2.3. Change in the pH of AMD as a Function of Adsorbent Dosage and Its Influence on Cr(VI) Adsorption

Adsorption of Cr(VI) varies as a function of the pH. In dissolved form, Cr(VI) can be present in any of the different forms H_2CrO_4, $HCrO_4^-$, CrO_4^{2-} or $Cr_2O_7^{2-}$ [4]. At low pH, the H^+ ions tend to protonate at the surface of adsorbent, resulting in a positively charged surface, which in turn has strong affinity for the negatively charged $HCrO_4^-$ [3]. At higher pH, a decrease in proton concentration leads to a negatively charged adsorbent surface which has less affinity for the adsorption of $HCrO_4^-$. At higher pH, interferences from OH^- ions may lead to lower removal efficiency of Cr(VI). Increased amounts of OH^- increases the competition between Cr(VI) and OH^- for occupying exchange sites in absorbent pore [60]. A similar pH dependent trend was also observed by a number of researchers for the Cr(VI) removal by various adsorbents [1,3,34,61,62]. At the adsorbent dosage of 10 g in 200 mL of AMD, the maximum pH levels attained by CEM I, FA, zeolite and GGBS were 12.0, 8.4, 4.8 and 9.2, respectively, as seen in Figure 3. At the higher adsorbent dosage of 60 g in 200 mL of AMD, the respective pH levels attained were significantly higher, giving 13.2, 10.1, 6.7 and 10.6 for CEM I, FA, zeolite and GGBS. In all cases, however, the pH rise was rapid and complete within 15 min of contact between AMD and the adsorbents, which also coincided with the maximum Cr(VI) removal levels achieved by zeolite and GGBS. In the AMD that was treated using CEM I and FA, the concentration of Cr(VI) strongly increased as pH of the AMD increased—a concern attributed to the overriding effect of the leaching of chromium from the absorbents into AMD. Cr(VI) in cement emanates from sources such as refractory bricks, fuels, and the chromium alloys; Chromium is present in coal mainly as trivalent chromium (Cr(III)). During the combustion of coal, Cr is usually oxidized from Cr(III) to Cr(VI). When exposed to water, Cr(VI) may leach out from the adsorbents [63]. Maximum Cr(VI) concentration levels of 4.27 mg/L and 0.558 mg/L were attained at pH levels of 13.6/8.77 of the treated mine water, under the dosage of 60 g of CEM I/FA in 200 mL of AMD, respectively. In a study of Cr(VI) removal from aqueous systems, Kantar et al. [64] reported that Cr(VI) reduction efficiency decreased with increasing solution pH. In contrast, Cr(VI) reduction efficiency increased with increasing solution

pH when GGBS was used as an adsorbent. This is because GGBS's activation is strongly dependent on pH values. Enhanced Cr(VI) reduction by GGBS is achieved at pH values higher than 11.5 [20]. The effects of increased alkalinity on efficient removal of Cr(VI) by GGBS was confirmed by the XRD/SEM results in Section 3.4.

3.2.4. Removal Efficiencies

The RE levels of Cr(VI) removal were determined for the various adsorbents, as summarised in Table 2. For each adsorbent dosage, the average equilibrium concentration of Cr(VI) was calculated for the contact durations of 15 to 300 min. The average Ce was then used in the calculation of RE as per Equation (5). It can be seen in Table 2 that the GGBS adsorbent gave the highest RE, achieving 100% removal of Cr(VI) followed by 76% removal by zeolite. CEM I or FA did not remove or reduce Cr(VI) concentration, but these adsorbents instead increased the chromium levels in the treated AMD, thus giving negative RE values which apparently were also very high. At the dosage of 10 g of adsorbent in 200 mL of AMD, CEM I and FA gave the RE values of −4781% and −1229%, respectively. The high Cr(VI) levels in the CEM I- and FA-treated AMD are a result of undesirable leaching behaviours of the two adsorbents.

Table 2. Removal Efficiency (RE) levels for Cr(VI) removal by Portland cement, fly ash, natural zeolite and ground granulated blast-furnace slag.

Adsorbent	Parameter	Dosage of Adsorbent in 200 mL of AMD			
		6 g of Adsorbent	10 g of Adsorbent	30 g of Adsorbent	60 g of Adsorbent
CEM I	RE (%)	−7519	−4781	−5305	−10,067
FA	RE (%)	−402	−1229	−990	−1174
Zeolite	RE (%)	76	71	66	75
GGBS	RE (%)	48	93	100	95

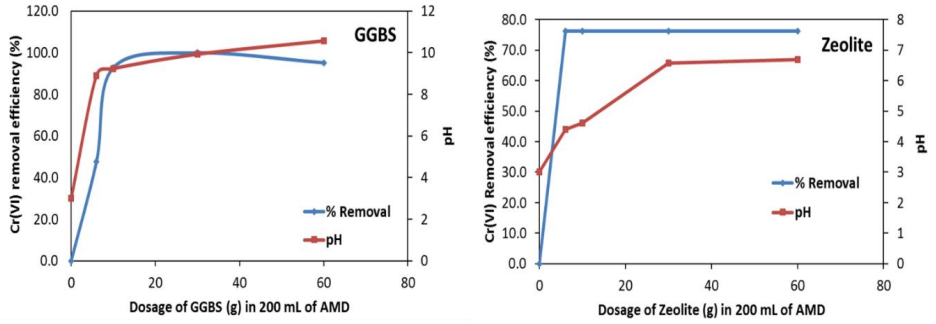

Figure 3. Influence of adsorbent dosage on pH and removal efficiency.

3.2.5. Isotherm Models

The Langmuir and Freundlich isotherm models were used to describe the equilibrium relationship between Cr(VI) and the adsorbents (zeolite and ground granulated blast-furnace slag). Correlation coefficient values are presented in Table 3.

Langmuir Isotherm

The correlation coefficients R^2 for the linear plot were >0.99 indicating that the experimental data of Cr(VI) adsorption using both adsorbents fitted well with the Langmuir isotherm model, as can be seen in Figure 4. Langmuir isotherm assumes monolayer adsorption on a homogenous surface [36]. The Langmuir dimensionless constant separation factor RL, was used to predict favourability of the isotherm. If RL < 1, then adsorption is favourable, while RL > 1 represents unfavourable adsorption, and RL = 0 irreversible process. According to the obtained results, RL was found to be 0.782 for GGBS, showing favourable adsorption of Cr(VI) by GGBS under the study conditions. RL value for zeolite was 0.999, indicating linear adsorption of Cr(VI) by zeolite.

Freundlich Isotherm

The linear form of Freundlich model equation is reported in Figure 5 for zeolite and GGBS, respectively. The R^2 values were 0.998 and 0.973 for zeolite and GGBS, respectively, indicating good correlation between the experimental data and Freundlich adsorption models for Cr(VI). Both the zeolite and GGBS possess high adsorption capacity for Cr(VI). The Freundlich equation can also be used to determine the adsorption intensity, 1/n, where n is an indicator of the change of intensity of the adsorption process—a value of n above 1 (n > 1) indicates favourable adsorption. A value of n below 1 (n < 1) indicates poor adsorption characteristics [65]. Our results showed n = 0.596 for zeolite, indicating poor adsorption of Cr(VI) by zeolite. The calculated n value for adsorption of Cr(VI) by GGBS was 1.187, showing good efficiency for Cr(VI) adsorption by GGBS adsorbent. The Freundlich model was found to fit the Cr(VI) adsorption better than the Langmuir model for both adsorbents, suggesting a multilayer adsorption of Cr(VI) on a heterogeneous surface. Other studies also reported that the Freundlich model described a much better fit than the Langmuir model in relation to Cr(VI) adsorption [37,38].

Table 3. Langmuir and Freundlich adsorption isotherm models determined for the adsorbents.

Adsorbent	Langmuir		Freundlich	
Zeolite	q_m (mg/g)	0.0262	n	0.596
	K_L (L/mg)	−31.58	K	125.81
	R_L	0.999	R^2	0.998
	R^2	0.965		
GGBS	q_m (mg/g)	0.0144	n	1.187
	K_L (L/mg)	4.729	K	1.311×10^{-4}
	R_L	0.782	R^2	0.973
	R^2	0.955		

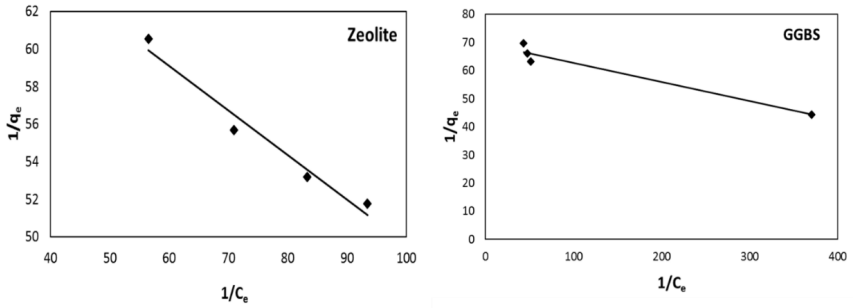

Figure 4. Langmuir model for adsorption of Cr(VI) onto zeolite and GGBS.

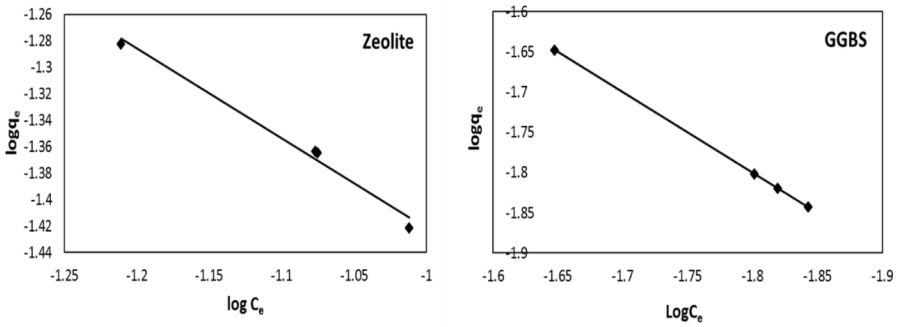

Figure 5. Freundlich model for adsorption of Cr(VI) onto zeolite and GGBS.

Comparison of Different Adsorbents for Cr(VI) Ions Removal

The maximum adsorption capacities of various adsorbents are presented in Table 4. By comparison, it was found that zeolite and GGBS were also able to efficiently remove Cr(VI) ions from aqueous media. Most adsorbents presented on Table 4 have been chemically modified to achieve high adsorption capacities. In the current study, maximum adsorption capacities were obtained without modifying the adsorbents and the adsorption conditions.

Table 4. Comparison of maximum removal capacity of Cr(VI) by various adsorbents.

Adsorbent	Qmax (mg/g)	Reference
Zeolite	0.0262 (76% removal)	Present study
GGBS	0.0144 (100% removal)	Present study
Activated carbon	72.46	[35]
Dolachar	0.904	[65]
Zeolite modified ZVI	2.49	[66]
Illite carbon nanocomposite	0.57	[67]
Activated Akadama clay	2.17	[68]

3.3. Cr(VI) Leaching Tests

Column tests were conducted to determine the leaching behaviour of Cr(VI) from CEM I, FA and GGBS. After 320 days of the experiment, the concentration of Cr(VI) for CEM1, FA and GGBS concrete samples was 0.184, 0.069 and 0.059 mg/L, respectively (Figure 6). CEM I and FA showed higher leachability of Cr(VI) that exceeded the recommended maximum concentration specified by the World Health Organisation (WHO) of 0.05 mg/L, and therefore poses an environmental risk. This is in agreement with adsorption experiments that showed elevated Cr(VI) levels in the AMD following its treatment using CEM I or FA. Hartwich and Vollpracht [69] reported that higher chromium content in cement results in higher pore solution concentrations and a higher release during leaching.

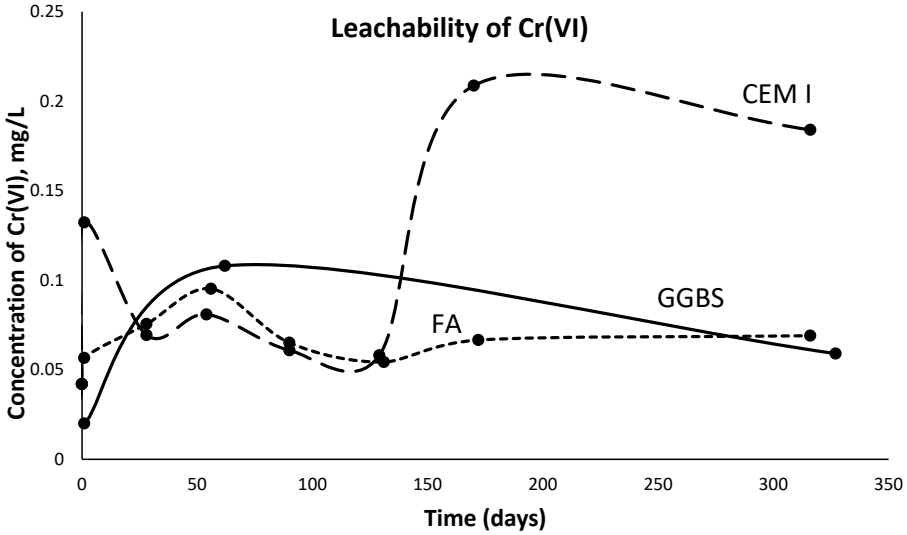

Figure 6. Concentrations of Cr(VI) leached from CEM1, GGBS and FA adsorbents.

3.4. Characterisation and FTIR Analysis

The XRD pattern of raw zeolite, as given in Figure 7a, identified the dominant minerals present to be the low-crystallised clinoptilolite ($(Na,K,Ca)_{2–3}Al_3(Al,Si)_2Si_{13}O_{36}·12H_2O$), quartz ($SiO_2$), and mordenite ($Al_2Si_{10}O_{24}·7H_2O$). In the reacted zeolite (Figure 7a), mordenite disappeared while a new phase muscovite appeared, indicating the transformation of the former to the latter phase. The co-existence of mordenite with the clinoptilolite in zeolites, was also observed by Diale et al. [70]. The high SiO_2

and Al_2O_3 in the zeolite adsorbent (Table 1) is responsible for its hydrophilic nature, an important property for adsorption of contaminants [71]. The cations Na, K, Ca and Mg found in zeolites generally, give the adsorbent its cation exchange capacity [16]. Figure 7b gives the XRD patterns of GGBS before and after its exposure to AMD. The wide hump between the 25° and 35° two-theta angles, shows that the GGBS was characteristically amorphous. The diffraction peak observed at the 30° two-theta angle of unreacted GGBS was identified as calcium carbonate ($CaCO_3$), most likely from the small amounts of limestone typically present in GGBS. It may be recalled that GGBS is a by-product of pig iron production from a mixture of limestone and forsterite or dolomite in some cases [72]. It can also be seen that the reaction between GGBS and AMD resulted in a significant formation of gypsum. GGBS is mainly composed of SiO_2, Al_2O_3 and CaO, as shown in Table 1. Again, the dissolution of CaO releases Ca ions, which combine with the SO_4^{2-} in the AMD solution and/or sulphuric acid from pyrite oxidation, leading to the formation of gypsum [47].

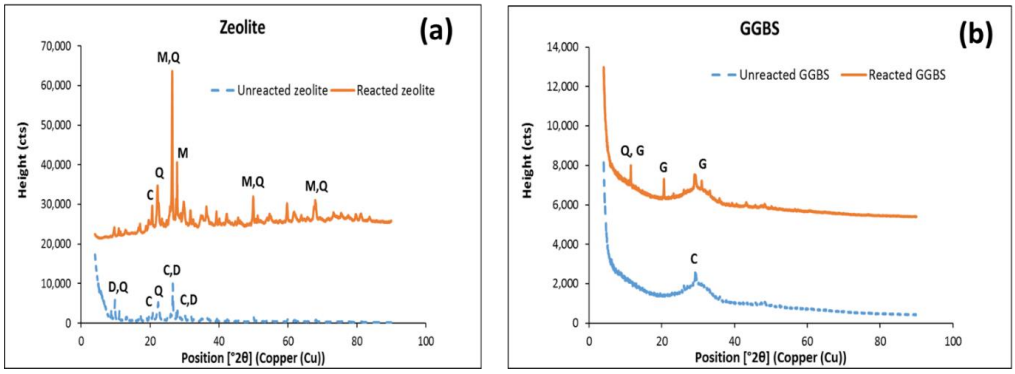

Figure 7. XRD spectra of (**a**) zeolite before and after reaction, (**b**) ground granulated blast-furnace slag (GGBS) before and after reaction with acid mine drainage: C—clinoptilolite; D—mordenite; G—gypsum, H—calcium carbonate/calcium oxide, M—muscovite, Q—quartz.

Figure 8a is an SEM micrograph of unreacted zeolite, showing clustered crystals of clinoptilolite plates. These structures provide a large surface area for fast and efficient adsorption of contaminants by the zeolite through ion exchange between cations of the adsorbent and contaminants in the mine water, including chromium [16,73]. The exchangeable ions Ca, K, Na found in unreacted zeolite as seen in the EDS of Figure 8b, could no longer be detected in the reacted zeolite, as evident in Figure 8c,d, indicating the occurrence of ion exchange between cations in zeolite and the positively charged ions in the mine water [73]. Jorfi et al. [60] reported that in aqueous solutions, chromium form oxyanions. At low pH values, these oxyanions are adsorbed onto the positively charged functional groups of zeolite. Therefore, the negatively charged Cr(VI) ions reduce the cationic exchange capacity and favour adsorption onto zeolite. The SEM micrograph of unreacted GGBS given in Figure 9a shows predominantly irregular particles of the slag. Figure 9b gives the EDS spectra for unreacted GGBS showing high content of C, Ca, Mg, Al and Si which are typical constituents of GGBS. When the CaO and MgO in GGBS (Table 1) react with water to form $Ca(OH)_2$ and $Mg(OH)_2$, respectively, an alkaline environment develops. With the resulting increase in pH, cement hydration products such as $Ca(OH)_2$, calcium-silicate-hydrate (C-S-H) and ettringite are formed [47]. These hydration products have a large specific surface area that provides physical sorption and co-precipitation sites for heavy metal ions such as Cr(VI) [20]. Cr(VI) may have also co-precipitated with gypsum, which was identified as the dominant product formed from the reaction of GGBS with AMD. GGBS particles also had a large surface area and high porosity levels, both of which promote metal sorption. Figure 9c gives the SEM micrograph of reacted GGBS showing an accumulation of gypsum inside an existing pore. The EDS for the reacted GGBS, as given in Figure 9d, shows a remarkable decrease in intensity levels of Ca^{2+}, Al^{3+} and Si^{4+} suggesting their consumption from the slag during AMD treatment.

FTIR spectra of the reacted and unreacted natural zeolite are given in Figure 10a, indicating the complex formations between the contaminants in AMD and different functional groups of the adsorbent. It can be seen that adsorption of contaminants was particularly associated with the silicon oxide (Si–O), the carboxylate anion (C=O) and hydroxyl (–OH) groups [74]. The spectrum of the unreacted zeolite indicates the presence of Si–O symmetric bands of quartz with a double peak at the wavenumbers 778 to 797 cm^{-1}, which majorly shifted to a single peak at 797 cm^{-1} of the reacted zeolite. The –OH group in the unreacted zeolite shows a signal at 2988 cm^{-1} which also shifted to form a strong broad band between 3264 cm^{-1} and 3395 cm^{-1}, denoting strong stretching vibrations in the reacted zeolite. Both the Si–O and –OH groups show the shifting of bands to higher numbers, indicating the adsorption of relatively lighter contaminant elements by the functional groups. The –OH group in the reacted zeolite also gave a strong increase and broadening of transmittance. The carboxylate C=O stretching at 1634 cm^{-1} showed no major shift but gave a strong increase and broadening of its transmittance peak. The observed broadening of the peaks belonging to the –OH and C=O groups in reacted zeolite, indicates an increase in contaminant concentrations and possible formation of crystalline phases, which points to chemisorption through cation exchange. In Figure 10b, the FTIR spectra of unreacted GGBS exhibit a band between wavenumbers 876 cm^{-1} and 963 cm^{-1}, representing stretching vibrations of the $AlO_4{}^{-1}$ group along with the related antisymmetric stretching vibrations of (Al)–O, respectively. The weak band at wavenumber 714 cm^{-1} is ascribed to Si–O–Si(Al) bridges, linked or related to the SiO_4 tetrahedral [75,76]. The transmittance wavenumbers (876 to 963, 714 cm^{-1}) observed in the unreacted slag were strongly reduced in the reacted GGBS, which may indicate the role of Al and Si towards effective contaminant removal by slag [76]. In a study of chromite and slag interactions by Lee and Nassaralla [77], it was reported that a replacement of Al_2O_3 in slag by SiO_2, reduced Cr(VI) formation. It was further shown that use of calcium silicate slags led to the formation of much smaller levels of Cr(VI) from chromite, while calcium aluminate slags gave very high chromium levels. The strong band at 1477 cm^{-1} indicates the presence of C–O stretching mode of calcite, with no role in contaminant adsorption as there was no major shift or change in its transmittance peak.

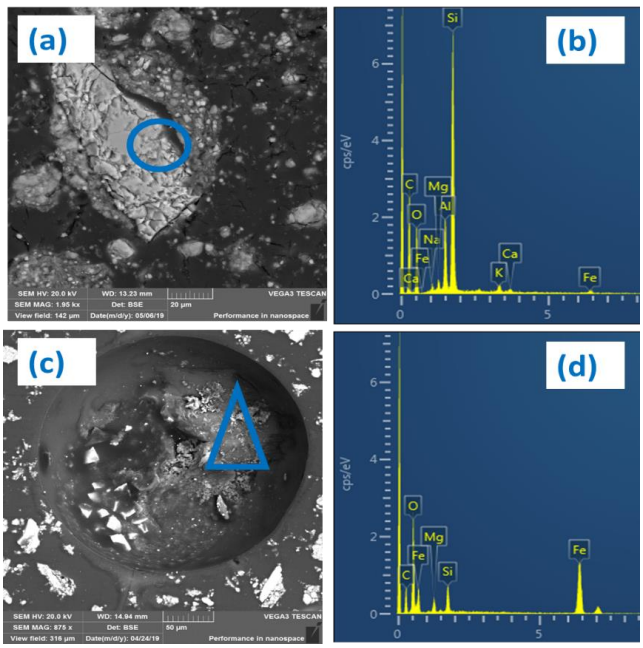

Figure 8. SEM–EDS of zeolite before and after the reaction with acid mine drainage: (**a**) micrograph of unreacted zeolite, (**b**) EDS spectra taken at a point selected with a circle in (**a**), (**c**) micrograph of reacted zeolite, (**d**) EDS spectra taken at a point selected with a triangle in (**c**).

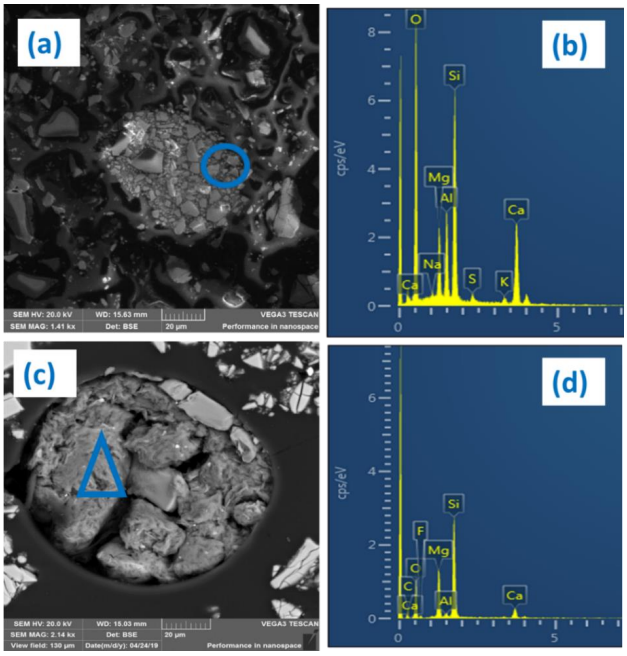

Figure 9. SEM–EDS of GGBS before and after reaction with acid mine drainage: (**a**) micrograph of unreacted GGBS, (**b**) EDS spectra taken at a point selected with a circle in (**a**), (**c**) micrograph of reacted GGBS, (**d**) EDS spectra taken at a point selected with a triangle in (**c**).

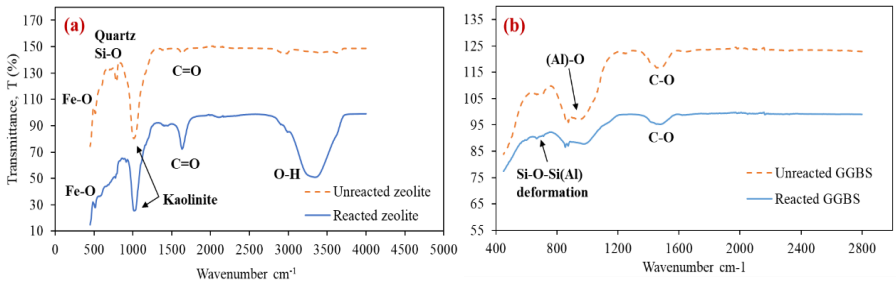

Figure 10. FTIR spectra of (**a**) zeolite before and after reaction, (**b**) ground granulated blast-furnace slag (GGBS) before and after reaction with acid mine drainage.

4. Conclusions

An investigation was conducted on Portland cement, fly ash (FA), natural zeolite and ground granulated blast-furnace slag (GGBS), as adsorbents for Cr(IV) removal from acid mine drainage (AMD). The following findings have been drawn.

1. Effective removal of Cr(VI) from AMD was achieved using at least 6 g of zeolite or 30 g of GGBS in 200 mL of AMD, giving the removal efficiency levels of 76% and 100%, respectively. In both cases, effective Cr(VI) removal was attained within 15 min of contact between the adsorbents and AMD.
2. In the converse, CEM I and FA strongly increased the Cr(VI) concentrations in AMD to levels far exceeding the permissible limits prescribed in national water standards, a concern attributed to leaching of the chromium present in the adsorbents into AMD.
3. The Freundlich model correlated best with Cr(VI) adsorption data, for both zeolite and GGBS, suggesting a multilayer adsorption of Cr(VI) on the surface of the adsorbents.
4. XRD and SEM analysis revealed high SiO_2 and Al_2O_3 in zeolite, which was responsible for its hydrophilic nature. Core-shell spheres and clustered crystals observed, confirmed the large surface area of zeolite that could lead to a fast and efficient adsorption of Cr(VI).

5. Cr(VI) removal, when using GGBS, can be attributed to its adsorption onto the surface of GGBS. Hydration products formed provided physical sorption and co-precipitation sites for Cr(VI). Cr(VI) may have also co-precipitated with gypsum, which was identified as the dominant product formed from the reaction of GGBS with AMD.
6. FTIR showed changes in O–H and C–O functional groups of zeolite and GGBS after CR(VI) adsorption, which is an indication of decationised adsorbents.
7. Zeolite and GGBS were found to be effective adsorbents for Cr(VI) removal and may be used as partial cement replacement materials in systems that employ pervious concrete technology for AMD treatment.

Author Contributions: Conceptualisation, A.N.S.; methodology, A.N.S., M.B.; investigation, A.N.S.; writing—original draft preparation, A.N.S.; writing—review and editing, A.N.S., M.B. All authors have read and agreed to the published version of the manuscript.

Funding: This research was funded by the National Research Foundation (NRF) of South Africa (grant numbers 96800, 116811).

Conflicts of Interest: The authors declare no conflict of interest.

References

1. Miretzky, P.; Cirelli, A.F. Cr(VI) and Cr(III) removal from aqueous solution by raw and modified lignocellulosic materials: A review. *J. Hazard. Mater.* **2010**, *180*, 1–19. [CrossRef] [PubMed]
2. Gheju, M. Decontamination of hexavalent chromium-polluted waters: Significance of metallic iron technology. In *Enhancing Cleanup of Environmental Pollutants*; Volume 2. Non-Biological Approaches; Anjum, N., Gill, S., Tuteja, N., Eds.; Springer International Publishing: Cham, Switzerland, 2017; pp. 209–254. [CrossRef]
3. Pradhan, D.; Sukla, L.B.; Sawyer, M.; Rahman, P.K.S.M. Recent bioreduction of hexavalent chromium in wastewater treatment: A review. *J. Ind. Eng. Chem.* **2017**, *55*, 1–20. [CrossRef]
4. Cherdchoo, W.; Nithettham, S.; Charoenpanich, J. Removal of Cr(VI) from synthetic wastewater by adsorption onto coffee ground and mixed waste tea. *Chemosphere* **2019**, *221*, 758–767. [CrossRef] [PubMed]
5. Divsholi, B.S.; Lim, T.Y.D.; Teng, S. Durability Properties and Microstructure of Ground Granulated Blast Furnace Slag Cement Concrete. *Int. J. Concr. Struct. Mater.* **2014**, *8*, 157–164. [CrossRef]
6. Hawileh, R.A.; Abdalla, J.A.; Fardmanesh, F.; Shahsana, P.; Khalili, A. Performance of reinforced concrete beams cast with different percentages of GGBS replacement to cement. *Arch. Civ. Mech. Eng.* **2017**, *17*, 511–519. [CrossRef]
7. Wu, Y.-H.; Huang, R.; Tsai, C.-J.; Lin, W.-T. Recycling of Sustainable Co-Firing Fly Ashes as an Alkali Activator for GGBS in Blended Cements. *Materials* **2015**, *8*, 784–798. [CrossRef]
8. De Medeiros, M.H.F.; Raisdorfer, J.W.; Filho, J.H.; Medeiros-Junior, R.A. Partial replacement and addition of fly ash in Portland cement: Influences on carbonation and alkaline reserve. *J. Build. Pathol. Rehabilit.* **2017**, *2*, 1165. [CrossRef]
9. Tchadjie, L.N.; Ekolu, S.O. Enhancing the reactivity of aluminosilicate materials toward geopolymer synthesis. *J. Mater. Sci.* **2017**, *53*, 4709–4733. [CrossRef]
10. Zhao, S.; Chen, Z.; Shen, J.; Qu, Y.; Wang, B.; Wang, X. Enhanced Cr(VI) removal based on reduction-coagulation-precipitation by NaBH 4 combined with fly ash leachate as a catalyst. *Chem. Eng. J.* **2017**, *322*, 646–656. [CrossRef]
11. Jones, S.N.; Cetin, B. Evaluation of waste materials for acid mine drainage remediation. *Fuel* **2017**, *188*, 294–309. [CrossRef]
12. Mushtaq, F.; Zahid, M.; Bhatti, I.A.; Nasir, S.; Hussain, T. Possible applications of coal fly ash in wastewater treatment. *J. Environ. Manag.* **2019**, *240*, 27–46. [CrossRef] [PubMed]
13. Zaetang, Y.; Wongsa, A.; Sata, V.; Chindaprasirt, P. Use of coal ash as geopolymer binder and coarse aggregate in pervious concrete. *Constr. Build. Mater.* **2015**, *96*, 289–295. [CrossRef]
14. Soto-Pérez, L.; Hwang, S. Mix design and pollution control potential of pervious concrete with non-compliant waste fly ash. *J. Environ. Manag.* **2016**, *176*, 112–118. [CrossRef] [PubMed]

15. Zanin, E.; Scapinello, J.; De Oliveira, M.; Rambo, C.L.; Franscescon, F.; Freitas, L.; De Mello, J.M.M.; Fiori, M.A.; Oliveira, J.V.; Magro, J.D. Adsorption of heavy metals from wastewater graphic industry using clinoptilolite zeolite as adsorbent. *Process. Saf. Environ. Prot.* **2017**, *105*, 194–200. [CrossRef]
16. Limper, D.; Fellinger, G.; Ekolu, S.O. Evaluation and microanalytical study of ZVI/scoria zeolite mixtures for treating acid mine drainage using reactive barriers—Removal mechanisms. *J. Environ. Chem. Eng.* **2018**, *6*, 6184–6193. [CrossRef]
17. Silva, B.; Figueiredo, H.; Quintelas, C.; Neves, I.; Tavares, M. Improved biosorption for Cr(VI) reduction and removal by Arthrobacter viscosus using zeolite. *Int. Biodeterior. Biodegrad.* **2012**, *74*, 116–123. [CrossRef]
18. Gaffer, A.K.; Alkahlawy, A.A.; Aman, D. Magnetic zeolite-natural polymer composite for adsorption of chromium (VI). *Egypt. J. Pet.* **2017**, *26*, 995–999. [CrossRef]
19. Adam, M.R.; Salleh, N.M.; Othman, M.H.D.; Matsuura, T.; Ali, M.H.; Othman, M.H.D.; Ismail, A.F.; Rahman, M.A.; Othman, M.H.D. The adsorptive removal of chromium (VI) in aqueous solution by novel natural zeolite based hollow fibre ceramic membrane. *J. Environ. Manag.* **2018**, *224*, 252–262. [CrossRef]
20. Bae, S.; Hikaru, F.; Kanematsu, M.; Yoshizawa, C.; Noguchi, T.; Yu, Y.-S.; Ha, J. Removal of Hexavalent Chromium in Portland Cement Using Ground Granulated Blast-Furnace Slag Powder. *Materials* **2017**, *11*, 11. [CrossRef]
21. Erdem, E.; Güngörmüş, H.; Kılınçarslan, R. The investigation of some properties of cement and removal of water soluble toxic chromium(VI) ion in cement by means of different reducing agents. *Constr. Build. Mater.* **2016**, *124*, 626–630. [CrossRef]
22. Barrera-Díaz, C.E.; Lugo, V.L.; Bilyeu, B. A review of chemical, electrochemical and biological methods for aqueous Cr(VI) reduction. *J. Hazard. Mater.* **2012**, *223*, 1–12. [CrossRef] [PubMed]
23. Yoshinaga, M.; Ninomiya, H.; Al Hossain, M.A.; Sudo, M.; Akhand, A.A.; Ahsan, N.; Alim, A.; Khalequzzaman, M.; Iida, M.; Yajima, I.; et al. A comprehensive study including monitoring, assessment of health effects and development of a remediation method for chromium pollution. *Chemosphere* **2018**, *201*, 667–675. [CrossRef] [PubMed]
24. Islam, A.; Angove, M.J.; Morton, D.W. Recent innovative research on chromium (VI) adsorption mechanism. *Environ. Nanotechnol. Monit. Manag.* **2019**, *12*, 100267. [CrossRef]
25. Wise, J.T.; Shi, X.; Zhang, Z. Toxicology of Chromium(VI). *Encycl. Environ. Health* **2019**, 1–8. [CrossRef]
26. Chao, H.-P.; Wang, Y.-C.; Tran, H.N. Removal of hexavalent chromium from groundwater by Mg/Al-layered double hydroxides using characteristics of in-situ synthesis. *Environ. Pollut.* **2018**, *243*, 620–629. [CrossRef]
27. International Agency for Research on Cancer (IARC). *IARC Monographs of the Evaluation of the Carcinogenic Risk of Chemicals to Humans*; Chromium, Nickel and Welding: Lyon, France, 1990; Volume 49, p. 687.
28. U.S. Environmental Protection Agency (USEPA). *IRIS, Toxicological Review of Hexavalent Chromium: 2010 External Review Draft*; U.S. Environmental Protection Agency: Washington, WA, USA, 2010.
29. World Health Organization (WHO). *Guidelines for Drinking-Water Quality*, 3rd ed.; World Health Organization: Geneva, Switzerland, 2004; p. 540.
30. Sinha, V.; Manikandan, N.A.; Pakshirajan, K.; Chaturvedi, R. Continuous removal of Cr(VI) from wastewater by phytoextraction using Tradescantia pallida plant based vertical subsurface flow constructed wetland system. *Int. Biodeterior. Biodegrad.* **2017**, *119*, 96–103. [CrossRef]
31. Pakade, V.E.; Tavengwa, N.T.; Madikizela, L.M. Recent advances in hexavalent chromium removal from aqueous solutions by adsorptive methods. *RSC Adv.* **2019**, *9*, 26142–26164. [CrossRef]
32. Anastopoulos, I.; Bhatnagar, A.; Bikiaris, D.N.; Kyzas, G.Z. Chitin Adsorbents for Toxic Metals: A Review. *Int. J. Mol. Sci.* **2017**, *18*, 114. [CrossRef]
33. Hokkanen, S.; Bhatnagar, A.; Sillanpää, M. A review on modification methods to cellulose-based adsorbents to improve adsorption capacity. *Water Res.* **2016**, *91*, 156–173. [CrossRef]
34. Parlayıcı, Ş.; Pehlivan, E. Comparative study of Cr(VI) removal by bio-waste adsorbents: Equilibrium, kinetics, and thermodynamic. *J. Anal. Sci. Technol.* **2019**, *10*, 15. [CrossRef]
35. Ramirez, A.; Ocampo-Pérez, R.; Giraldo, S.; Padilla-Ortega, E.; Florez, E.; Acelas, N. Removal of Cr (VI) from an aqueous solution using an activated carbon obtained from teakwood sawdust: Kinetics, equilibrium, and density functional theory calculations. *J. Environ. Chem. Eng.* **2020**, *8*, 103702. [CrossRef]
36. Shi, Y.; Shan, R.; Lu, L.; Yuan, H.; Jiang, H.; Zhang, Y.; Chen, Y. High-efficiency removal of Cr(VI) by modified biochar derived from glue residue. *J. Clean. Prod.* **2020**, *254*, 119935. [CrossRef]

37. Mishra, S.P.; Ghosh, M.R. Use of silver impregnated activated carbon (SAC) for Cr(VI) removal. *J. Environ. Chem. Eng.* **2020**, *8*, 103641. [CrossRef]
38. Ahmadi, A.; Foroutan, R.; Esmaeili, H.; Tamjidi, S. The role of bentonite clay and bentonite clay@MnFe2O4 composite and their physico-chemical properties on the removal of Cr(III) and Cr(VI) from aqueous media. *Environ. Sci. Pollut. Res.* **2020**, *27*, 1–14. [CrossRef] [PubMed]
39. Achary, P.G.R.; Ghosh, M.R.; Mishra, S.P. Insights into the modeling and application of some low cost adsorbents towards Cr(VI) adsorption. *Mater. Today Proc.* **2020**, in press. [CrossRef]
40. Jerin, V.M.; Remya, R.; Mariyam, T.; Jaya, T.V. Investigation on the Removal of toxic Chromium Ion from Waste Water using Fe_2O_3 Nanoparticles. *Mater. Today Proc.* **2019**, *9*, 27–31. [CrossRef]
41. Zhao, R.; Zhou, Z.; Zhao, X.; Jing, G. Enhanced Cr(VI) removal from simulated electroplating rinse wastewater by amino-functionalized vermiculite-supported nanoscale zero-valent iron. *Chemosphere* **2019**, *218*, 458–467. [CrossRef]
42. Scholz, M.; Grabowiecki, P. Review of permeable pavement systems. *Build. Environ.* **2007**, *42*, 3830–3836. [CrossRef]
43. Ekolu, S.O.; Azene, F.Z.; Diop, S. A concrete reactive barrier for acid mine drainage treatment. *Proc. Inst. Civ. Eng. Water Manag.* **2014**, *167*, 373–380. [CrossRef]
44. Nnadi, E.O.; Newman, A.P.; Coupe, S.J.; Mbanaso, F.U. Stormwater harvesting for irrigation purposes: An investigation of chemical quality of water recycled in pervious pavement system. *J. Environ. Manag.* **2015**, *147*, 246–256. [CrossRef]
45. Solpuker, U.; Sheets, J.M.; Kim, Y.; Schwartz, F.W. Leaching potential of pervious concrete and immobilization of Cu, Pb and Zn using pervious concrete. *J. Contam. Hydrol.* **2014**, *161*, 35–48. [CrossRef] [PubMed]
46. Holmes, R.; Hart, M.; Kevern, J.T. Heavy metal removal capacity of individual components of permeable reactive concrete. *J. Contam. Hydrol.* **2017**, *196*, 52–61. [CrossRef]
47. Shabalala, A.N.; Ekolu, S.O.; Diop, S.; Solomon, F. Pervious concrete reactive barrier for removal of heavy metals from acid mine drainage—Column study. *J. Hazard. Mater.* **2017**, *323*, 641–653. [CrossRef] [PubMed]
48. Shabalala, A.; Ekolu, S. Quality of water recovered by treating acid mine drainage using pervious concrete adsorbent. *Water SA* **2019**, *45*, 638–647. [CrossRef]
49. Shabalala, A.; Ekolu, S.O. Assessment of the Suitability of Mine Water Treated with Pervious Concrete for Irrigation Use. *Mine Water Environ.* **2019**, *38*, 798–807. [CrossRef]
50. Boudaghpour, S.; Biglarijoo, N.; Ahmadi, S. A review on the existence of chrome in cement and environmental remedies to control its effects. *Int. J. Geol.* **2012**, *6*, 62–67.
51. Potgieter, S.; Panichev, N.; Potgieter, J.; Panicheva, S. Determination of hexavalent chromium in South African cements and cement-related materials with electrothermal atomic absorption spectrometry. *Cem. Concr. Res.* **2003**, *33*, 1589–1593. [CrossRef]
52. American Public Health Association (APHA). *Standard Methods for the Examination of Water and Wastewater*, 18th ed.; American Public Health Association: Washington, WA, USA, 1992; pp. 3–59.
53. Yousefi, A.; Matavos-Aramyan, S. Mix Design Optimization of Silica Fume-Based Pervious Concrete for Removal of Heavy Metals from Wastewaters. *Silicon* **2018**, *10*, 1737–1744. [CrossRef]
54. Kebede, T.G.; Mengistie, A.A.; Dube, S.; Nkambule, T.T.; Nindi, M.M. Study on adsorption of some common metal ions present in industrial effluents by Moringa stenopetala seed powder. *J. Environ. Chem. Eng.* **2018**, *6*, 1378–1389. [CrossRef]
55. Ayanda, O.S.; Fatoki, O.S.; Adekola, F.A.; Ximba, B.J. Characterization of Fly Ash Generated from Matla Power Station in Mpumalanga, South Africa. *J. Chem.* **2012**, *9*, 1788–1795. [CrossRef]
56. Sawyer, T. *Assessment of the Suitability of Ground Granulated Arc Furnace Slag as a Cementitious Extender*; Technical Report; 2012; p. 14. Available online: https://www.researchgate.net/publication/318490127 (accessed on 14 September 2020).
57. Eštoková, A.; Palaščáková, L.; Singovszka, E.; Holub, M. Analysis of the Chromium Concentrations in Cement Materials. *Procedia Eng.* **2012**, *42*, 123–130. [CrossRef]
58. Environmental Protection Agency (EPA). The Environment (Protection) Act, Rev. 1998, General Standards for Discharge of Environmental Pollutants Part-A: Effluents, Schedule VI, Gazette of India, S.O. 844(E), Revised, G.S.R. 7. 1986. Available online: http://www.envfor.nic.in/legis/env/env4.html (accessed on 5 September 2019).

59. National Water Act (NWA). *Discharge Limits and Conditions Set Out in the National Water Act, Government Gazette No. 20526, 8 October*; Department of Water Affairs (DWA): Pretoria, South Africa, 1999.
60. Jorfi, S.; Ahmadi, M.J.; Pourfadakari, S.; Jaafarzadeh, N.; Soltani, R.D.C.; Akbari, H. Adsorption of Cr(VI) by Natural Clinoptilolite Zeolite from Aqueous Solutions: Isotherms and Kinetics. *Pol. J. Chem. Technol.* **2017**, *19*, 106–114. [CrossRef]
61. Chen, S.; Zhang, J.; Wang, X. Removal of Hexavalent Chromium from Contaminated Water by Chinese Herb-Extraction Residues. *Water Air Soil Pollut.* **2017**, *228*, 693. [CrossRef]
62. Mishima, K.; Du, X.; Sekiguchi, S.; Kano, N. Experimental and Theoretical Studies on the Adsorption and Desorption Mechanisms of Chromate Ions on Cross-Linked Chitosan. *J. Funct. Biomater.* **2017**, *8*, 51. [CrossRef] [PubMed]
63. Huggins, F.; Rezaee, M.; Honaker, R.; Hower, J. On the removal of hexavalent chromium from a Class F fly ash. *Waste Manag.* **2016**, *51*, 105–110. [CrossRef]
64. Kantar, C.; Ari, C.; Keskin, S.; Dogaroglu, Z.G.; Karadeniz, A.; Alten, A. Cr(VI) removal from aqueous systems using pyrite as the reducing agent: Batch, spectroscopic and column experiments. *J. Contam. Hydrol.* **2015**, *174*, 28–38. [CrossRef]
65. Panda, H.; Tiadi, N.; Mohanty, M.; Mohanty, C. Studies on adsorption behavior of an industrial waste for removal of chromium from aqueous solution. *S. Afr. J. Chem. Eng.* **2017**, *23*, 132–138. [CrossRef]
66. Dang, H.; Zhang, Y.; Du, P. Enhanced removal of soluble Cr(VI) by using zero-valent iron composite supported by surfactant-modified zeolites. *Water Sci. Technol.* **2014**, *70*, 1398–1404. [CrossRef]
67. Wang, G.; Wang, S.; Sun, W.; Sun, Z.; Zheng, S. Synthesis of a novel illite@carbon nanocomposite adsorbent for removal of Cr(VI) from wastewater. *J. Environ. Sci.* **2017**, *57*, 62–71. [CrossRef]
68. Zhao, Y.; Qi, W.; Chen, G.; Ji, M.; Zhang, Z. Behavior of Cr(VI) removal from wastewater by adsorption onto HCl activated Akadama clay. *J. Taiwan Inst. Chem. Eng.* **2015**, *50*, 190–197. [CrossRef]
69. Hartwich, P.; Vollpracht, A. Influence of leachate composition on the leaching behaviour of concrete. *Cem. Concr. Res.* **2017**, *100*, 423–434. [CrossRef]
70. Diale, P.P.; Muzenda, E.; Zimba, J. A study of South African natural zeolites properties and applications. In Proceedings of the World Congress on Engineering and Computer Science, San Francisco, CA, USA, 19–21 October 2011.
71. Olegario, E.; Pelicano, C.M. Characterization of Philippine Natural Zeolite and its Application for Heavy Metal Removal from Acid Mine Drainage (AMD). *Key Eng. Mater.* **2017**, *737*, 407–411. [CrossRef]
72. Suresh, D.; Nagaraju, K. Ground Granulated Blast Slag (GGBS) in concrete—A Review. *J. Mech. Civ. Eng.* **2015**, *12*, 76–82.
73. Basaldella, E.I.; Vazquez, P.G.; Iucolano, F.; Caputo, D. Chromium removal from water using LTA zeolites: Effect of pH. *J. Colloid Interface Sci.* **2007**, *313*, 574–578. [CrossRef] [PubMed]
74. Naiya, T.; Singha, B.; Das, S. *FTIR Study for the Cr(VI) Removal from Aqueous Solution Using Rice Waste, Int. Conf. on Chemistry and Chemical Process, IPCBEE Vol. 10*; IACSIT Press: Singapore, 2011; pp. 114–119.
75. Mihailova, I.; Dimitrova, S.; Mehandjiev, D. Effect of the thermal treatment on the Pb(II) adsorption ability of blast-furnace slag. *J. Chem. Technol. Metall.* **2013**, *48*, 72–79.
76. Yasipourtehrani, S.; Strezov, V.; Evans, T. *Investigation of Phosphate Removal Capability of Blast-Furnace Slag in Wastewater Treatment, Scientific Reports*; Department of Environmental Sciences. Macquarie University: Sydney, Australia, 2019; p. 9.
77. Lee, Y.; Nassaralla, C.L. Formation of hexavalent chromium by reaction between slag and magnesite-chrome refractory. *Met. Mater. Trans. A* **1998**, *29*, 405–410. [CrossRef]